Synthesis of the Neutral $(CuF(NC_5H_5)_4)_2NbOF_5$ Cluster

Alexander J. Norquist, Margaret E. Welk, Charlotte L. Stern, and Kenneth R. Poeppelmeier*

Department of Chemistry, Northwestern University, Evanston, Illinois 60208-3113

Received February 15, 2000. Revised Manuscript Received April 13, 2000

Composition space diagrams can be used to study the stability and variety of mixed transition metal oxide fluorides prepared under hydro(solvato)thermal conditions. Prior to this work the neutral $(CuF(NC_5H_5)_4)_2NbOF_5$ cluster had not been observed but it was expected because of the nucleophilic character of the oxygen and trans fluorine in the $[NbOF_5]^{2-}$ species. $[H_3O]_2[(CuF(NC_5H_5)_4)_2NbOF_5][F]_2$, a compound containing the 2:1 (Cu:Nb) cluster, was synthesized from the concentration variables, $[CuO{\cdot}0.5\ Nb_2O_5]$, $[(HF)_x{\cdot}$pyridine], and $[H_2O]$, by adding a fourth, [pyridine], and extending the composition space from a two-dimensional triangle to a three-dimensional prism. Crystal Data: $[H_3O]_2[(CuF(NC_5H_5)_4)_2NbOF_5][F]_2$, tetragonal, space group $I4_1/acd$ (no. 142), with $a = 24.691(1)$ Å, $c = 14.556(1)$ Å, $Z = 8$.

Introduction

Polar distortions in early transition metal oxide fluoride anions such as $[MOF_5]^{2-}$ (M = Nb, Ta) resemble the out of center distortion in $LiNbO_3$,which is the origin of its unique nonlinear optical properties. Orienting these anions into noncentrosymmetric structures requires understanding the conditions necessary to crystallize them without introducing an inversion center. This required knowing the residual negative charge on each ligand in the anion.[1] Coordination is preferential to those ligands with the most residual negative charge, which are then the most nucleophilic. Recently bond valence calculations were used to show that the $[NbOF_5]^{2-}$ anion directs coordination in a trans fashion.[2] Neutral 1:1 (Cu:Nb) chains of $Cu(py)_4NbOF_5$ (py = NC_5H_5) and anionic 1:2 clusters of $[Cu(py)_4(NbOF_5)_2]^{2-}$ were observed in the $CuO{\cdot}0.5Nb_2O_5/(HF)_x{\cdot}$pyridine/$H_2O$ composition space. The neutral 2:1 (Cu:Nb) cluster, $(CuF(py)_4)_2NbOF_5$ (see Figure 1), did not form at these conditions despite the anion's expected favorable trans coordination.

Composition space diagrams, which plot reaction products as a function of the mole fractions for each of three reactants, are constructed by analyzing the solid product, thus revealing the crystallization fields.[2,3] Recently several reports[4−6] have discussed incorporating the reactant/solvent ratio as a variable in the synthesis. The resulting composition prism is analogous to multiple composition space diagrams. This technique was employed to synthesize the compound, $[H_3O]_2[(CuF(py)_4)_2NbOF_5][F]_2$, which could not form in the previously reported $CuO{\cdot}0.5Nb_2O_5/(HF)_x{\cdot}$pyridine/$H_2O$ composition space.

Experimental Section

Caution. $(HF)_x{\cdot}$pyridine is toxic and corrosive!

Materials. CuO (99%, Aldrich), Nb_2O_5 (99.99%, Aldrich), pyridine (99.8%, anhydrous, Aldrich), and $(HF)_x{\cdot}$pyridine (pyridinium poly(hydrogen fluoride), 70 wt %, Aldrich) were used as received. Reagent amounts of deionized H_2O were used in the synthesis.

Synthesis. Previously the synthesis and structure of $[pyH]_2[Cu(py)_4(NbOF_5)_2]$ and $Cu(py)_4NbOF_5$ were reported.[3] $[H_3O]_2[(CuF(py)_4)_2NbOF_5][F]_2$ was synthesized by adding 0.0269 g (3.39×10^{-4} mol) of CuO, 0.0451 g (3.39×10^{-4} mol) of Nb_2O_5, 0.8708 g (3.31×10^{-3} mol) of $(HF)_x{\cdot}$pyridine, 0.9653 g (1.22×10^{-2} mol) of pyridine, and 0.0740 g (4.11×10^{-3} mol) of deionized water to a Teflon (fluoro-ethylene-propylene) "pouch."[7] The pouches were sealed and placed into a 2000-mL autoclave (Parr) filled with 600 mL of deionized water. The autoclave was sealed and heated to 150 °C for 24 h and then cooled to room temperature over an additional 24 h. The pouches were removed from the autoclave and opened in air. Products were recovered by filtration. $[H_3O]_2[(CuF(py)_4)_2NbOF_5][F]_2$ was recovered as thin blue needles in 40% yield based on Cu.

Crystallographic Determination. Relevant crystallographic data, selected atomic coordinates, and isotropic thermal parameters are listed in Tables 1 and 2. All calculations were preformed using the TEXSAN crystallographic software package from Molecular Structure Corp.[8] The structure was solved by direct methods[9] and expanded using Fourier techniques.[10]

Crystal Structure of $[H_3O]_2[(CuF(py)_4)_2NbOF_5][F]_2$. On the basis of systematic absences and successful solution and refinement of the structure, the space group was determined to be $I4_1/acd$ (no. 142). Disorder in $[NbOF_5]^{2-}$ anion results in F1 and O1 being constrained to occupy the same position. All copper, niobium, oxygen, and fluorine positions except O1 and F1 were refined using anisotropic thermal parameters. All

* Corresponding author

(1) Heier, K. R.; Norquist, A. J.; Wilson, C. G.; Stern, C. L.; Poeppelmeier, K. R. *Inorg. Chem.* **1998**, *37*, 76.
(2) Norquist, A. J.; Heier, K. R.; Stern, C. L.; Poeppelmeier, K. R. *Inorg. Chem.* **1998**, *37*, 6495.
(3) Harrison, W. T. A.; Dussack, L. L.; Jacobson, A. J. *J. Solid State Chem.* **1996**, *125*, 234.
(4) Halasyamani, P.; Willis, M. J.; Stern, C. L.; Lundquist, P. M.; Wong, G. K.; Poeppelmeier, K. R. *Inorg. Chem.* **1996**, *35*, 1367.
(5) Francis, R. J.; Halasyamani, P. S.; Bee, J. S.; O'Hare, D. *J. Am. Chem. Soc.* **1999**, *121*, 1609.
(6) Walker, S. M.; Halasyamani, P. S.; Allen, S.; O'Hare, D. *J. Am. Chem. Soc.* **1999**, *121*, 10513.
(7) Harrison, W. T. A.; Nenoff, T. M.; Gier, T. E.; Stucky, G. D.; *Inorg. Chem.* **1993**, *32*, 2437.

10.1021/cm0001354 CCC: $19.00
Published on Web 06/16/2000

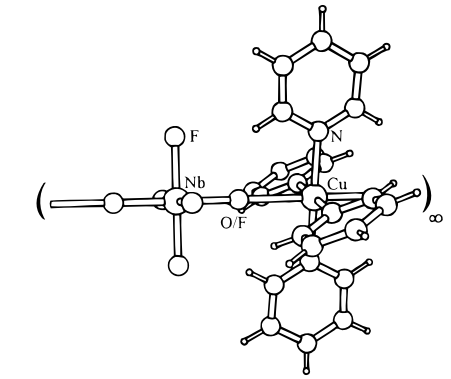

(a) Neutral 1:1 (Cu:Nb) Chain

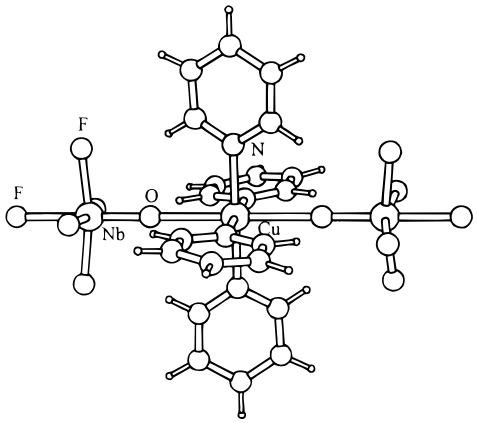

(b) Anionic 1:2 (Cu:Nb) Cluster

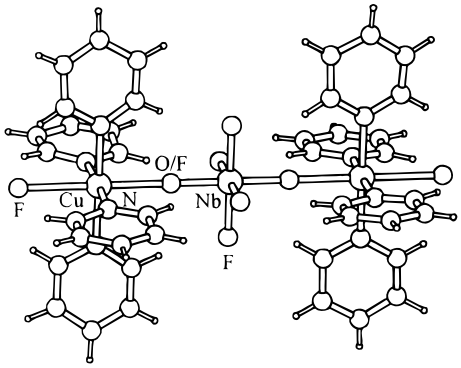

(c) Neutral 2:1 (Cu:Nb) Cluster

Figure 1. Examples of the three main structure types: (a) neutral chain, $Cu(py)_4NbOF_5$, (b) anionic cluster, $[Cu(py)_4(NbOF_5)_2]^{2-}$, and (c) neutral cluster, $(CuF(py)_4)_2NbOF_5$.

other non-hydrogen atoms were refined using isotropic thermal parameters because the crystal diffracted X-rays poorly. Only 806 of 3060 unique reflections were greater than 2σ. The lack of data prohibited the use of anisotropic thermal parameters on more sites. H13 was placed in an idealized 32 g position ($\sim$1/4, 0, 1/4) and its *x*-parameter refined. All other hydrogen atoms were located from the difference map and placed as nonrefined positions.

Table 1. Crystallographic Data for $[H_3O]_2[(CuF(py)_4)_2NbOF_5][F]_2$

$[H_3O]_2[(CuF(py)_4)_2NbOF_5][F]_2$	
empirical formula: $C_{40}H_{46}Cu_2NbF_8N_8O_3$	$T = -120(1)$ °C
fw 1077.84	$\lambda = 0.71069$ Å
space group $I4_1/acd$ (no. 142)	$\rho_{calcd} = 1.613$ g/cm^3
$a = 24.691(1)$ Å	$\rho_{obsd}{}^a = 1.600(4)$ g/cm^3
$c = 14.556(1)$ Å	$\mu = 12.89$ cm^{-1}
$V = 8873.5(9)$ Å^3	$R^b = 0.044$
$Z = 8$	$R_w{}^c = 0.032$

[a] Density measurements by flotation pycnometry at 25 °C. [b] $R = \Sigma||F_O| - |F_C||/\Sigma|F_O|$. [c] $R_w = [\Sigma(|F_O| - |F_C|)^2/\Sigma(F_O)^2]^{1/2}$.

Table 2. Selected Atomic Coordinates for $[H_3O]_2[(CuF(py)_4)_2NbOF_5][F]_2$

atom	site	*x*	*y*	*z*	B_{eq},[a] Å^2	occ
Nb	8b	0.00	0.25	0.125	2.00(2)	1
Cu	16f	0.12015(5)	0.1299	0.125	2.05(2)	1
F1	16f	−0.0550(3)	0.3050	0.125	1.4(2)	1/2
F2	16d	0.00	0.25	0.2577(4)	1.7(2)	1
F3	16f	0.0554(2)	0.3054	0.125	1.80(9)	1
F4	16f	0.1954(3)	0.0546	0.125	3.3(1)	1
F5	16f	0.3197(2)	−0.0697	0.125	6.8(2)	1
O1	16f	−0.0550(3)	0.3050	0.125	1.4(2)	1/2
O2	32g	0.2568(7)	−0.0077(6)	0.1744(7)	2.1(4)	1/2
N1	32g	0.1190(4)	0.1252(5)	−0.0148(4)	1.6(2)	1
N2	32g	0.1797(3)	0.1873(3)	0.1219(8)	1.6(1)	1
H11	16f	0.28	−0.0332	0.125	1.7(1)	1
H12	16f	0.23	0.0207	0.125	1.7(1)	1
H13	32g	0.264(5)	0.0	0.25	1.7(1)	1/2

[a] $B_{eq} = (8/3)\pi^2(U_{11}(aa^*)^2 + (U_{22}(bb^*)^2 + (U_{22}(bb^*)^2 + (U_{33}(cc^*)^2 + 2U_{12}aa^*bb^* \cos\gamma + 2U_{13}aa^*cc^* \cos\beta + 2U_{23}bb^*cc^* \cos\alpha)$.

Spectroscopic Measurements. Mid-infrared (400−4000 cm^{-1}) spectra were collected using a Bio-Rad FTS-60 FTIR spectrometer operating at a resolution of 2 cm^{-1}.

Susceptibility. The temperature dependence of the magnetic moment for powdered single crystals (mass = 0.0484 g) was collected with a dc Superconductivity Quantum Interference Device (SQUID) magnetometer from Quantum Design. After the powder was zero-field-cooled to 5 K, a 0.1 T field was applied and the magnetic moment was registered. The susceptibility values were calculated from the magnetic moment data using the Curie−Weiss law.

Results

Four composition space diagrams, shown in Figure 2, were constructed in the $CuO{\cdot}0.5Nb_2O_5/(HF)_x{\cdot}$pyridine/$H_2O$ system by varying the amount of solvent (pyridine) added from 0.5 to 2.0 g. In each case the total number of moles of reactants, CuO, 0.5 Nb_2O_5, $(HF)_x{\cdot}$pyridine, and H_2O, was kept constant at 0.0075. The crystallization fields of $Cu(py)_4NbOF_5$, $[pyH]_2[Cu(py)_4(NbOF_5)_2]$, and $[H_3O]_2[(CuF(py)_4)_2NbOF_5][F]_2$ dominate in different regions through the series of diagrams.

Each composition space diagram contains two common regions, one at high metal oxide mole fraction and one at high $(HF)_x{\cdot}$pyridine mole fraction. At high metal oxide mole fraction there is not enough HF in the reaction to completely dissolve the oxides. Unreacted metal oxide is present throughout the reaction, providing many nucleation sites that cause the products to precipitate as small cystallites, unsuitable for single-crystal diffraction. The reaction products in this region are unreacted metal oxides and poorly crystalline

(8) *TEXSAN*: *Crystal Structure Analysis Package*; Molecular Structure Corp.: The Woodlands, TX, 1985 and 1992.

(9) Sheldrick, G. M. SHELXS86. In *Crystallographic Computing 3*; Sheldrick, G. M., Kruger, C., Goddard, R., Eds.; Oxford University Press: Oxford, U.K., 1985; pp 175−189.

(10) Beurskens, P. T.; Admiraal, G.; Beurskens, G.; Bosman, W. P.; de Gelder, R.; Israel, R.; Smits, J. M. M. *The DIRDIF_94 program system*; Technical Report of the Crystallography Laboratory; University of Nijmegen: Nijmegen, The Netherlands, 1994.

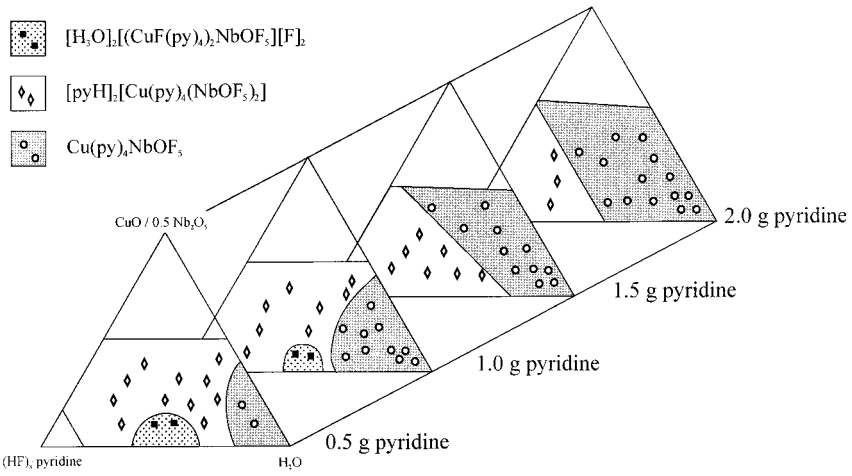

Figure 2. Composition prism for the $CuO{\cdot}0.5Nb_2O_5/(HF)_x{\cdot}$pyridine/$H_2O$ system. Each region represents the crystallization field of the respective compound. The white areas represent the 2:1 (Cu:Nb) anionic cluster compound, $[pyH]_2[Cu(py)_4(NbOF_5)_2]$, the shaded areas represent the 1:1 (Cu:Nb) neutral chain compound, $Cu(py)_4NbOF_5$, and the spotted areas represent the 2:1 (Cu:Nb) neutral cluster compound, $[H_3O]_2[(CuF(py)_4)_2NbOF_5][F]_2$. The boundaries separating each crystallization field are not sharp. In adjacent areas, a mixture of products is often observed. The amount of pyridine added in each reaction is listed beside each composition space diagram. Points represent individual reaction compositions.

products that were not characterized further. In the high $(HF)_x{\cdot}$pyridine region no solid products form and all species remain soluble owing to the high HF mole fraction.

0.5 g Pyridine. The $(CuO{\cdot}0.5Nb_2O_5/(HF)_x{\cdot}$pyridine/$H_2O)$:0.5 g pyridine composition space diagram consists of three crystallization fields. $Cu(py)_4NbOF_5$, the neutral chain, forms in very low HF concentrations. $[H_3O]_2[(CuF(py)_4)_2NbOF_5][F]_2$, the neutral cluster, forms at very low metal oxide concentrations. $[pyH]_2[Cu(py)_4(NbOF_5)_2]$, the anionic cluster, forms over the remaining region of the diagram.

1.0 g Pyridine. The $(CuO{\cdot}0.5Nb_2O_5/(HF)_x{\cdot}$pyridine/$H_2O)$:1.0 g pyridine composition space diagram consists of three crystallization fields. The neutral chain forms in moderate to low HF concentrations. The neutral cluster forms at very low metal oxide concentrations. The anionic cluster forms over the rest of the composition space diagram.

1.5 g Pyridine. Two crystallization fields exist in the $(CuO{\cdot}0.5Nb_2O_5/(HF)_x{\cdot}$pyridine/$H_2O)$:1.5 g pyridine composition space. At high $(HF)_x{\cdot}$pyridine concentrations the anionic cluster forms where the probability of coordination by $[pyH]^+$ is high. The neutral chain forms in lower HF concentrations where the relative $[pyH]^+$ concentration is low with respect to the $[Cu(py)_4]^{2+}$ concentration.

2.0 g Pyridine. Two crystallization fields exist in the $(CuO{\cdot}0.5Nb_2O_5/(HF)_x{\cdot}$pyridine/$H_2O)$:2.0 g pyridine composition space. Over much of the composition space the neutral chain forms where the probability of coordination by $[pyH]^+$ is low. Only at much higher $(HF)_x{\cdot}$pyridine concentrations does the anionic cluster form.

$[H_3O]_2[(Cu(py)_4)_2NbOF_5][F]_2$. The neutral $(Cu(py)_4)_2NbOF_5$ cluster is constructed of a central $[NbOF_5]^{2-}$ anion coordinated by two $[CuF(py)_4]^{2+}$ cations in a trans fashion through the oxide, O1, and trans fluoride, F1, ligands. The central $[NbOF_5]^{2-}$ anion is crystallographically disordered, O1 and F1 are constrained to occupy the same position, and no out of center distortion by the Nb is observed in the $[NbOF_5]^{2-}$ octahedra. An elongated Nb thermal ellipsoid is observed along the F—Nb═O bond axis, consistent with a model in which the Nb occupies two sites.

The $(Cu(py)_4)_2NbOF_5$ clusters pack in the (0 0 1) planes in a "herringbone" pattern. Each plane is rotated 90° every *c*/4, resulting in a 4_1 screw axis. The packing creates channels parallel to the *c* axis. See Figure 4. Two-thirds of the channels are filled by the pyridine rings of the $[CuF(py)_4]^+$ cations. Oxonium molecules (H_3O^+) and fluoride (F^-) ions occupy the remaining channels in a hydrogen bonded network. The terminal fluoride ligand on each $[CuF(py)_4]^+$ cation hydrogen bonds to a oxonium molecule, which in turn hydrogen bonds to another uncoordinated fluoride ion. The central oxygen of each oxonium molecule, O2, is disordered over two sites, each $^1/_2$ occupied. See Figure 5. The orientation of the oxonium molecules in individual channels must be ordered, that is all the oxonium atoms must exhibit local order, as demonstrated in Figure 5. A disordered model is impossible within a single channel because the terminal hydrogen, H13, cannot be connected to two oxygens. The possibility of $[H_5O_2]^+$ residing in the channels was eliminated because the characteristic mode at 1900−1700 cm^{-1} is missing,[11] while the modes observed at 3430(2), 750(2), and 1604(2) cm^{-1} are indicative of $[H_3O]^+$.[12] The infrared spectrum of $[H_3O]_2[(CuF(py)_4)_2NbOF_5][F]_2$ confirms the presence of coordinated pyridine (1604 and 639 cm^{-1}) and the Nb═O stretch is observed at 909 cm^{-1}.

The fluoride ions which occupy the channels (F5) exhibit an abnormally large B_{eq} with respect to the other atoms; see Table 2. Partial occupation of this site has been eliminated as a possibility because the stoichiometry has been confirmed using elemental analysis. Elemental analysis found (calcd): C 44.32 (44.53), N 4.06 (4.26), H 10.25 (10.39), F 16.17 (15.86). The shortest contact distances from F5 are to H3 and H4 at 2.49 and 2.74 Å respectively, while the sum of the van der Waals radii of H and F is ∼2.7 Å. A figure showing these distances is available in the Supporting Information.

(11) Pavia, A. C.; Giguere, P. A. *J. Chem. Phys.* **1970**, *52*, 3551.
(12) Christe, K. O.; Charpin, P.; Soulie, E.; Bougon, R.; Fawcett. J.; Russell, D. R. *Inorg. Chem.* **1984**, *23*, 3756.

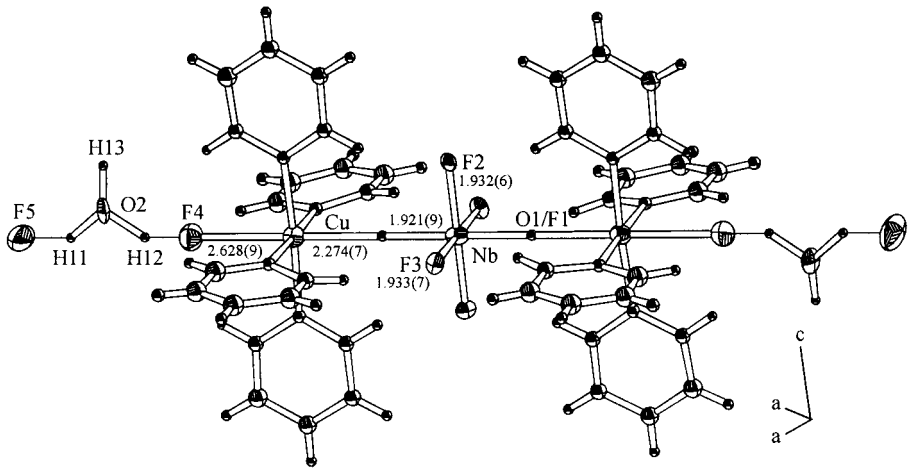

Figure 3. Thermal ellipsoid plot (50% probability) of $[H_3O]_2[(CuF(py)_4)_2NbOF_5][F]_2$. Selected bond lengths are included (Å).

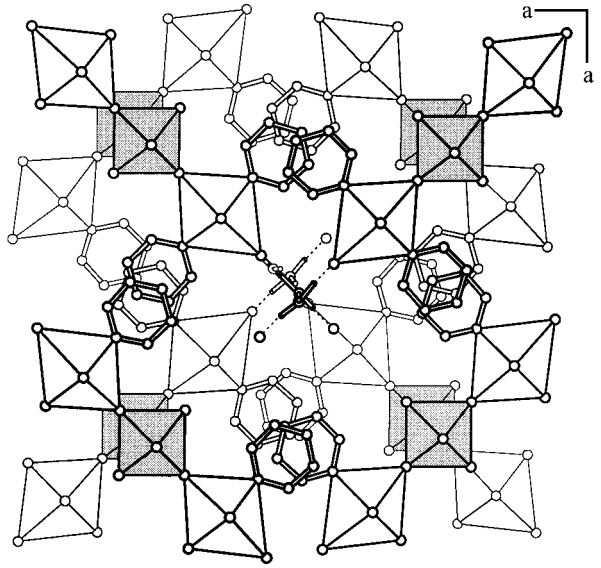

Figure 4. Packing diagram of $[H_3O]_2[(CuF(py)_4)_2NbOF_5][F]_2$. Shaded octahedra represent $[NbOF_5]^{2-}$, and unshaded octahedra represent $[CuF(py)_4]^+$. Pyridine rings not in the (0 0 1) plane have been removed for clarity. Dashed lines denote hydrogen bonding interactions.

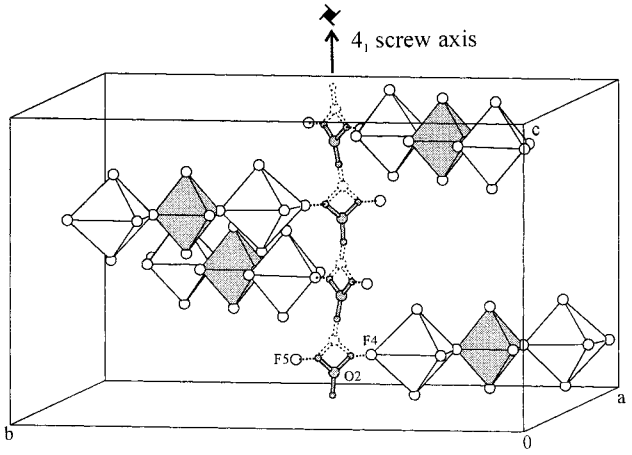

Figure 5. Hydrogen bonding in $[H_3O]_2[(CuF(py)_4)_2NbOF_5][F]_2$. Shaded octahedra represent $[NbOF_5]^{2-}$ and unshaded octahedra represent $[CuF(py)_4]^+$. The 4_1 screw axis can be observed in the 90° rotation of each $(CuF(py)_4)_2NbOF_5$ cluster every *c*/4. The shaded oxonium molecules represent the short-range order in the hydrogen bonding model. Including the dashed oxonium atoms demonstrates the disordered, macroscopic model. Pyridine rings have been removed for clarity.

The molar susceptibility has shown the sample to be a Curie paramagnet with a $\mu_{effc} = 1.8\ \mu_B$. The slope is in good agreement with isolated Cu^{2+} (d^9). The Weiss constant is very low, on the order of 0.1°, consistent with the shortest Cu − Cu distance of 8.38 Å.

Discussion

The $[NbOF_5]^{2-}$ anion directs coordination in a trans fashion through the oxide and trans fluoride ligands. In the $CuO{\cdot}0.5Nb_2O_5/(HF)_x{\cdot}$pyridine/$H_2O$/pyridine composition prism all three species shown in Figure 1 are favored because they each are based on trans coordination, the preferred arrangement, of the $[NbOF_5]^{2-}$ anion, yet the neutral $(CuF(py)_4)_2NbOF_5$ cluster was not previously observed. The neutral cluster was observed in other systems which employ anions with similar structure directing properties.[2] The nucleophilicity of the ligands in $[TaOF_5]^{2-}$ are very similar to those in $[NbOF_5]^{2-}$ as shown using bond valence calculations.[13] The neutral cluster, $[H_3O]_2[(CuF(py)_4)_2TaOF_5][F]_2$, forms in the $(CuO{\cdot}0.5Ta_2O_5/(HF)_x{\cdot}$pyridine/$H_2O$) composition space[2] implying that under appropriate conditions the 2:1 (Cu:Nb) neutral cluster should form.

Several conditions must be met to synthesize $[H_3O]_2[(CuF(py)_4)_2NbOF_5][F]_2$. First, conditions should favor the coordination of a $[F]^-$ ligand over a second $[NbOF_5]^{2-}$ anion to the $[Cu(py)_4]^{2+}$. Otherwise either the 1:1 chain, $Cu(py)_4NbOF_5$, or the 1:2 (Cu:Nb) anionic cluster, $[Cu(py)_4(NbOF_5)_2]^{2-}$ forms instead of the desired 2:1 (Cu:Nb) neutral cluster, $(CuF(py)_4)_2NbOF_5$. Second, pyridinium must not hydrogen bond to ligands on the $[NbOF_5]^{2-}$ anion. Pyridinium hinders the coordination of two $[Cu(py)_4]^{2+}$ cations around the $[NbOF_5]^{2-}$ anion, preventing the formation of $(CuF(py)_4)_2NbOF_5$. Third, $[H_3O]^+$ must be present in to fill the channels of the structure. A composition prism defined by $CuO{\cdot}0.5Nb_2O_5/(HF)_x{\cdot}$pyridine/$H_2O$/pyridine was constructed to access conditions where these three criteria could be met.

In the $(CuO{\cdot}0.5Nb_2O_5/(HF)_x{\cdot}$pyridine/$H_2O$):2.0 g pyridine composition space, the neutral chain dominates because the ratio of protonated pyridine to unprotonated

(13) Norquist, A. J.; Stern, C. L.; Poeppelmeier, K. R. *Inorg. Chem.* **1999**, *38*, 3448.

pyridine favors the formation of the 1:1 (Cu:Nb) neutral chain. The anionic cluster forms in higher $(HF)_x$·pyridine mole fractions where coordination of a $[pyH]^+$ is more probable. The neutral cluster does not form because coordination of a second $[NbOF_5]^{2-}$ anion to the $[Cu(py)_4]^{2+}$ cation is favored over a $[NbOF_5]^{2-}$ anion and a $[F]^-$ ligand.

In the $(CuO{\cdot}0.5Nb_2O_5/(HF)_x{\cdot}pyridine/H_2O)$:1.5 g pyridine composition space the ratio of protonated to unprotonated pyridine remains high over a wider region. Throughout this area the anionic cluster forms readily and the neutral chain recedes to area of lower $(HF)_x$·pyridine mole fraction. $[H_3O]_2[(CuF(py)_4)_2NbOF_5][F]_2$ is not yet observed because the equilibrium between a second $[NbOF_5]^{2-}$ anion coordinating to the $[Cu(py)_4]^{2+}$ as opposed to a $[F]^-$ ligand is shifted toward the coordination of a second $[NbOF_5]^{2-}$ anion.

The anionic cluster forms over the majority of the $(CuO{\cdot}0.5Nb_2O_5/(HF)_x{\cdot}pyridine/H_2O)$:1.0 g pyridine. In this system the ratio of protonated to unprotonated pyridine is high in all regions of the composition space diagram. In regions of high water concentration, where the mole fraction of $(HF)_x$·pyridine is low, $Cu(py)_4NbOF_5$ forms. The neutral cluster forms at very low metal oxide mole fractions, where both the $(HF)_x$·pyridine and H_2O mole fractions are high. All three conditions necessary for the neutral cluster's formation have been met in this small area of composition space.

In the $(CuO{\cdot}0.5Nb_2O_5/(HF)_x{\cdot}pyridine/H_2O)$:0.5 g pyridine system the crystallization field of $Cu(py)_4NbOF_5$ retreats further into the water corner of composition space. In this region the pyridinium/pyridine ratio is low, and the coordination of two $[Cu(py)_4]^{2+}$ cations versus one $[Cu(py)_4]^{2+}$ cation and one pyridinium around a $[NbOF_5]^{2-}$ anion is favored. The 2:1 (Cu:Nb) neutral cluster forms in the same region as in the $(CuO{\cdot}0.5Nb_2O_5/(HF)_x{\cdot}pyridine/H_2O)$:1.0 g pyridine diagram because all three necessary conditions have been met. The anionic cluster forms over large regions of these diagram because the pyridinium/pyridine ratio can remain high even with a decreasing $(HF)_x$·pyridine mole fraction, owing to the much lower amount of pyridine added to each reaction.

A composition prism clearly shows the dependence of a crystallization field on the mole fractions of the reactants and the reactant/solvent ratio compared to previous diagrams constructed with a fixed reactant/solvent ratio. Introducing the solvent concentration allowed the target phase, $[H_3O]_2[(CuF(py)_4)_2NbOF_5][F]_2$, to be synthesized and crystals grown. Composition prisms are useful because they clearly illustrate the crystallization fields present and their dependence on both the mole fractions of the reactants and the reactant/solvent ratio.

Acknowledgment. The authors gratefully acknowledge support from the National Science Foundation, Solid State Chemistry (Award No. DMR-9727516), and made use of Central Facilities supported by the MRSEC program of the National Science Foundation (Grant DMR-9632472) at the Materials Research Center of Northwestern University.

Supporting Information Available: An X-ray crystallographic file (in CIF format) and a magnetic susceptibility plot with accompanying data and a figure demonstrating selected contact distances (in PDF) This material is available free of charge via the Internet at http://pubs.acs.org.

CM0001354